Clinical Value of Optimized FLAIR Imaging at 7 Tesla: Neuroimaging Case Examples

Emilie Sleight[1,2], Jose Federico Ojeda Esparza[3], Gian Franco Piredda[4], Jürgen Herrler[5], Tom Hilbert[4,6,7], Karl-Olof Lövblad[3,8], Dimitrios Karampinos[1,2], Frédéric Grouiller[1,8,9], Felix T. Kurz[3,8]

[1] CIBM Center for Biomedical Imaging, Lausanne, Switzerland
[2] Laboratory of Magnetic Resonance Imaging Systems and Methods, Ecole Polytechnique Fédérale de Lausanne, Lausanne, Switzerland
[3] Division of Neuroradiology, Diagnostic Department, Geneva University Hospitals, Geneva, Switzerland
[4] Swiss Innovation Hub, Siemens Healthineers International AG, Lausanne, Switzerland
[5] Siemens Healthineers AG, Erlangen, Germany
[6] Department of Radiology, Lausanne University Hospital and University of Lausanne, Lausanne, Switzerland
[7] LTS5, Ecole Polytechnique Fédérale de Lausanne, Lausanne, Switzerland
[8] Department of Radiology and Medical Informatics, Faculty of Medicine, University of Geneva, Geneva, Switzerland
[9] Division of Radiology, Diagnostic Department, Geneva University Hospitals, Geneva, Switzerland

Introduction

Fluid-attenuated inversion recovery (FLAIR) is a widely used MRI contrast in clinical neuroimaging. This is due to its high sensitivity for detecting parenchymal lesions, particularly in regions adjacent to cerebrospinal fluid (CSF). By suppressing the CSF signal while preserving T2-weighted contrast, FLAIR improves lesion conspicuity in a wide range of neurological conditions. It is therefore recommended in the assessment of multiple neurological diseases, including multiple sclerosis [1, 2], epilepsy [3, 4], brain tumors [5], and neurodegenerative disorders such as dementia [6].

With the increasing availability of ultra-high-field MRI systems, imaging at 7 Tesla (7T) has created new opportunities for neuroimaging by providing a substantial gain in signal-to-noise ratio compared with lower field strengths [7, 8]. This gain enables higher spatial resolution and improved lesion detection, which is particularly attractive for diseases characterized by subtle or small lesions. Indeed, several studies have demonstrated increased lesion sensitivity at 7T compared with conventional field strengths [9, 10].

Despite these advantages, the clinical implementation of FLAIR at 7T remains challenging and many sites report suboptimal image contrast or limited robustness. These limitations are primarily related to increased specific absorption rate (SAR) [11], changes in tissue relaxation times that reduce contrast between gray and white matter [12, 13], and pronounced B_1^+ field inhomogeneities that can cause regional signal loss [11]. As a result, FLAIR is sometimes omitted from 7T clinical protocols, despite its established diagnostic value at lower field strengths.

This article presents an optimized 3D FLAIR sequence protocol designed to address these challenges on the 7T MAGNETOM Terra.X system. The clinical value is illustrated using selected neuroimaging cases.

FLAIR sequence optimization

At 7T, limitations in SAR restrict the use of 180° refocusing flip angles [11]. However, the 3D SPACE sequence uses variable refocusing flip angles, which substantially reduces SAR while preserving image quality and whole-brain coverage.

A further challenge for ultra-high-field MRI is the reduced intrinsic contrast between gray and white matter on FLAIR images, largely due to prolonged T1 and altered T2 relaxation times. To compensate for this effect, a T2-preparation module was added prior to the inversion recovery [13], with the preparation duration optimized to enhance tissue contrast on FLAIR images. Table 1 provides the parameters for the 7T 3D FLAIR SPACE sequence.

Finally, B_1^+ inhomogeneities at 7T can lead to regional signal loss, particularly in the temporal lobes, cerebellum, and brain stem, and are especially pronounced on FLAIR images. These effects were mitigated using parallel transmission (pTx) technology [14–16]. In this work, fast online-customized (FOCUS) pTx pulses were employed with an 8Tx32Rx head coil (Nova Medical, Wilmington, MA, USA), enabling improved flip-angle homogeneity across the brain with limited SAR exposure by designing subject-specific pTx pulses, resulting in more uniform image quality [17, 18].

Parameter	Value
Orientation	Sagittal
FOV (mm^3)	225 × 180 × 156
Resolution (mm^3)	0.7 × 0.7 × 0.7
Slices per slab	224
Acceleration	CAIPI 3 × 2 (shift 1)
TR (ms)	8000
Magnetization preparation	Non-sel. T2 prep. IR
T2 prep. duration (ms)	200
TI (ms)	1990
Flip angle mode	T2 variable
Tissue T1 (ms)	1500
Tissue T2 (ms)	50
TE (ms)	300
Echo spacing (ms)	4.28
Turbo factor	180
Bandwidth (Hz/Px)	751
RF pulse type	Low SAR
Gradient mode	Normal
Acquisition time (min:s)	8:18

Table 1: Parameters of the 7T FLAIR SPACE sequence with FOCUS pTx pulses.

Conclusion

The clinical cases presented here illustrate the added value of an optimized 7T 3D FLAIR SPACE protocol across a range of neurological pathologies. Compared to standard 3T imaging, 7T FLAIR provided improved lesion conspicuity, sharper lesion delineation, and enhanced visualization of subtle cortical and juxtacortical abnormalities.

In cases with indeterminate lesions, 7T FLAIR enabled the detection of small additional abnormalities that were not visible at 3T, potentially contributing to a more comprehensive assessment of lesion burden.

For suspected low-grade glioma in the temporal lobe, the use of pTx technology mitigated signal loss related to B_1^+ inhomogeneities in lower brain regions, which made it possible to detect the tumor at 7T. Compared with 3T FLAIR, ultra-high-field imaging provided improved delineation of cortical involvement and lesion margins, revealing features of cortical infiltration. This enhanced lesion characterization increased diagnostic confidence in distinguishing an infiltrative glioma from non-infiltrative juxtacortical white matter abnormalities, and may have implications for clinical decision-making.

Similarly, in a case of suspected multinodular and vacuolating neuronal tumors, 7T FLAIR enabled clearer delineation of lesion extent and revealed a characteristic multinodular, aggregated architecture of multiple juxta-cortical and subcortical hyperintense nodules that appeared more confluent on 3T imaging, thereby providing imaging features with potential diagnostic relevance.

In the context of epilepsy, 7T FLAIR demonstrated clear advantages in visualizing focal cortical dysplasia. This allowed more confident identification of abnormalities and more-targeted resection while minimizing the removal of adjacent non-pathological tissue.

These examples highlight the strength of optimized FLAIR imaging at 7T for pathologies where subtle changes or lesion extent are clinically relevant. Overall, with appropriate sequence and RF optimization, FLAIR imaging at 7T can be robustly integrated into clinical neuroimaging protocols. The resulting gains in lesion sensitivity and anatomical detail may provide clinically meaningful information beyond that available at 3T, supporting diagnosis, treatment planning, and patient management.

Case 1

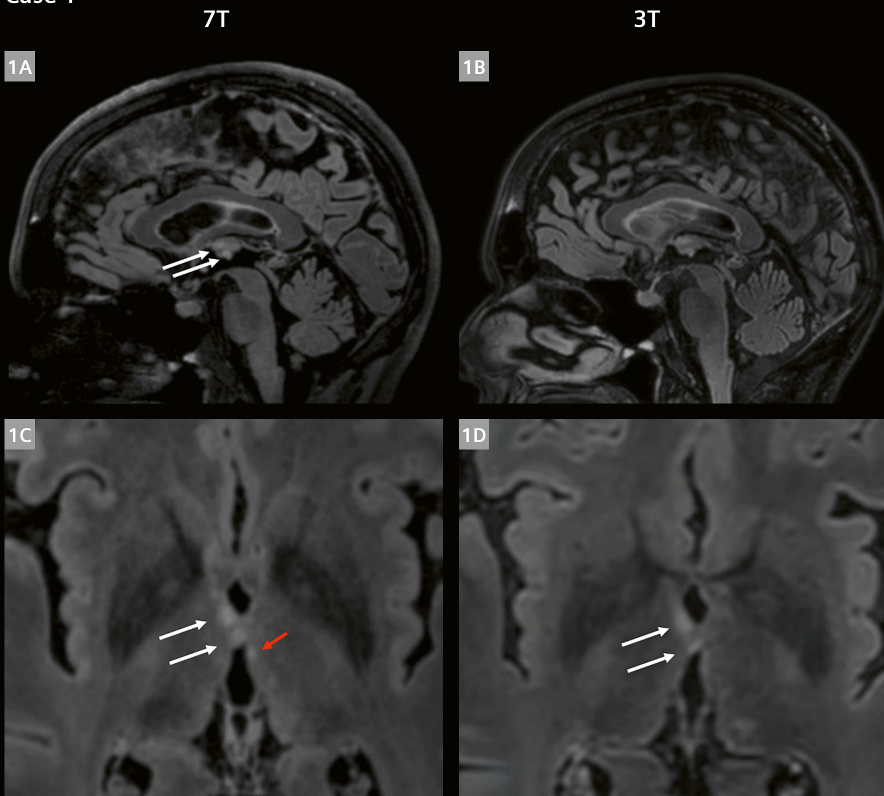

1 Bithalamic lesions of indeterminate origin in a 57-year-old patient. The FLAIR-hyperintense bithalamic lesions are well visible (white arrows) at both 7T **(1A, 1C)** and 3T **(1B, 1D)**, but are more conspicuous at 7T. **(1C)** A small lesion to the left of the third ventricle (red arrow) is only visible on 7T FLAIR, not on 3T FLAIR **(1D)**.

Case 2

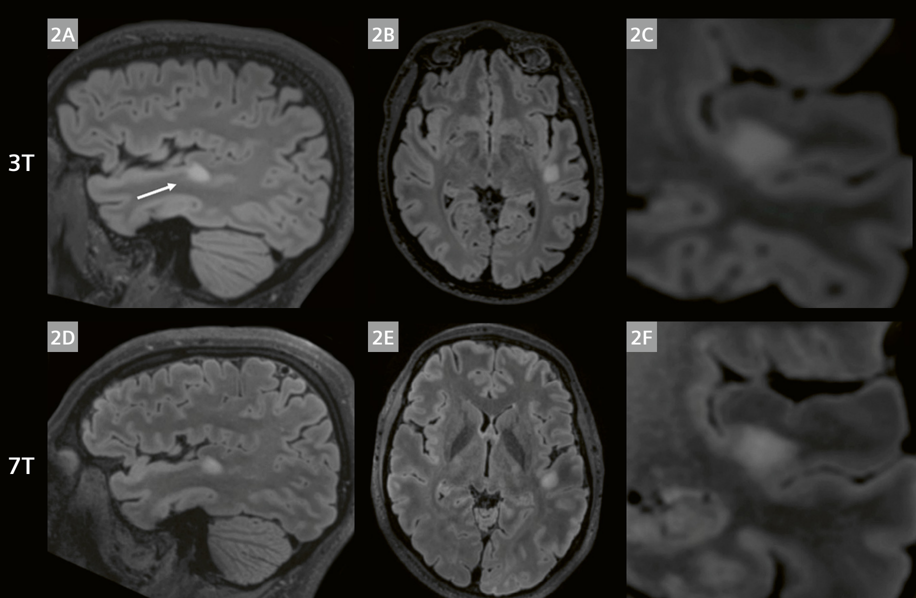

2 Suspected left temporal low-grade glioma. **(2A–2C)** 3T FLAIR-hyperintense left temporal lesion (white arrow) in **(2A)** sagittal, **(2B)** axial, and **(2C)** zoomed-in coronal orientations. **(2D–2F)** 7T images of the same lesion in **(2D)** sagittal, **(2E)** axial, and **(2F)** zoomed-in coronal orientations. Signal in the temporal lobe at 7T is only possible when using pTx pulses. Cortical infiltration was equivocal on 3T FLAIR, but more clearly delineated at 7T, thereby improving lesion characterization and diagnostic confidence when distinguishing an infiltrative lesion such as a low-grade glioma from non-infiltrative juxtacortical white matter abnormalities, and potentially informing surgical indication and planning.

Case 3

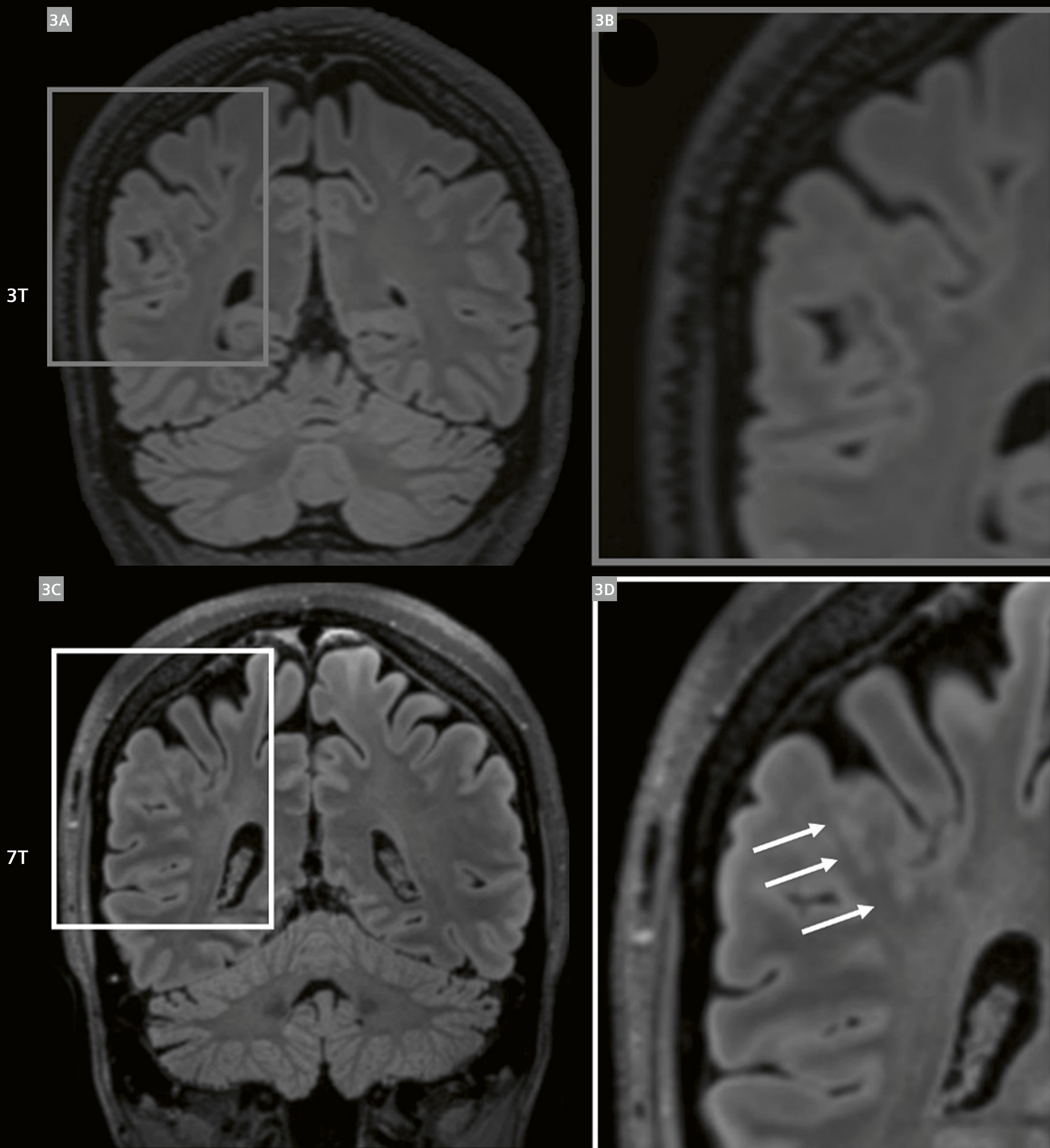

3 Suspicion of a multinodular and vacuolating neuronal tumor (MVNT) in the right superior parietal lobule. **(3A)** 3T FLAIR image in coronal orientation, with a magnified view of the superior parietal lobule subregion shown in **(3B)**. **(3C)** Corresponding 7T FLAIR image, with magnified view shown in **(3D)**, demonstrating multiple juxtacortical and subcortical hyperintense lesions. With 7T FLAIR, the extent of the lesion and its multinodular aggregated architecture are more clearly depicted, in contrast to the more confluent appearance on 3T, a pattern that can have diagnostic implications.

Case 4

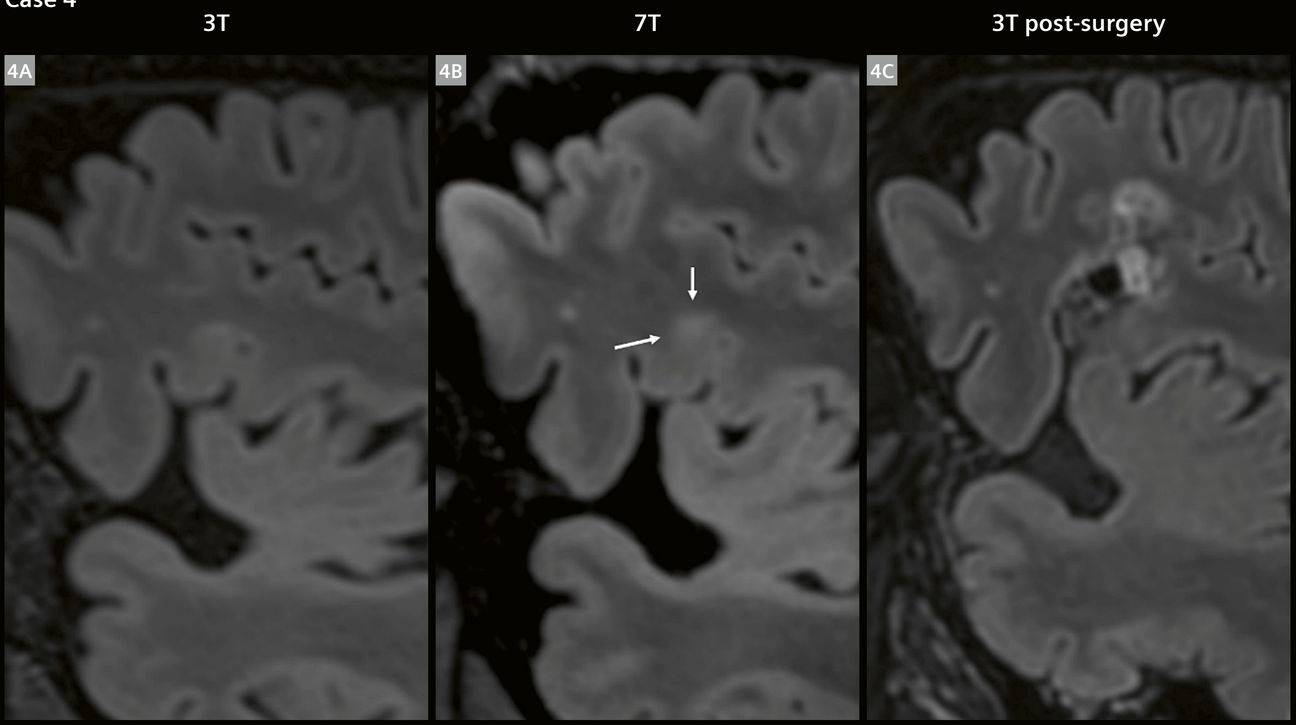

4 Left frontal focal cortical dysplasia type IIb. **(4A)** Magnified view of a 3T sagittal FLAIR image of a patient with focal epilepsy, retrospectively demonstrating subtle cortical and subcortical FLAIR-hyperintense changes involving the left inferior frontal gyrus (Brodmann area 45). **(4B)** 7T FLAIR image of the same area, which shows improved lesion delineation (white arrows) compared to 3T. This allowed for a more precise definition of the dysplastic cortex preoperatively, which facilitated a better targeted resection while minimizing removal of adjacent non-pathological tissue. **(4C)** 3T post-operative FLAIR image following resection of the cortical dysplasia (scan conducted three months after surgery).

Acknowledgments

We acknowledge the MRI Platform of the FCBG (Fondation Campus Biotech Geneva), and the CIBM Center for Biomedical Imaging, for providing expertise and resources to conduct this study. We also acknowledge research support from Siemens Healthineers.

References

1 Traboulsee A, Li DKB. Conventional MR imaging. Neuroimaging Clin N Am. 2008;18(4):651–673. [Multiple Sclerosis, Part I: Background and Conventional MRI].
2 Bakshi R, Ariyaratana S, Benedict RHB, Jacobs L. Fluid-Attenuated Inversion Recovery Magnetic Resonance Imaging Detects Cortical and Juxtacortical Multiple Sclerosis Lesions. Arch Neurol. 2001; 58(5):742–748.
3 Rüber T, David B, Elger CE. MRI in epilepsy: clinical standard and evolution. Curr Opin Neurol. 2018;31(2):223–231.
4 Opheim G, van der Kolk A, Markenroth Bloch K, Colon AJ, Davis KA, Henry TR, et al. 7T Epilepsy Task Force Consensus Recommendations on the Use of 7T MRI in Clinical Practice. Neurology. 2021; 96(7):327–341.
5 Upadhyay N, Waldman AD. Conventional MRI evaluation of gliomas. Br J Radiol. 2011;84 Spec No 2(Spec Iss 2):S107–11.
6 Theysohn JM, Kraff O, Maderwald S, Barth M, Ladd SC, Forsting M, et al. 7 tesla MRI of microbleeds and white matter lesions as seen in vascular dementia. J Magn Reson Imaging. 2011;33(4):782–91.
7 Uğurbil K. Magnetic Resonance Imaging at Ultrahigh Fields. IEEE Trans Biomed Eng. 2014;61(5):1364–1379.
8 van der Kolk AG, Hendrikse J, Zwanenburg JJ, Visser F, Luijten PR. Clinical applications of 7 T MRI in the brain. Eur J Radiol. 2013; 82(5):708–18.
9 Veersema TJ, Ferrier CH, van Eijsden P, Gosselaar PH, Aronica E, Visser F, et al. Seven tesla MRI improves detection of focal cortical dysplasia in patients with refractory focal epilepsy. Epilepsia Open. 2017;2(2):162–171.

10 Wang I, Oh S, Blümcke I, Coras R, Krishnan B, Kim S, et al. Value of 7T MRI and post-processing in patients with nonlesional 3T MRI undergoing epilepsy presurgical evaluation. Epilepsia. 2020; 61(11):2509–2520.
11 Barisano G, Sepehrband F, Ma S, Jann K, Cabeen R, Wang DJ, et al. Clinical 7 T MRI: Are we there yet? A review about magnetic resonance imaging at ultra-high field. Br J Radiol. 2019;92(1094): 20180492.
12 Rooney WD, Johnson G, Li X, Cohen ER, Kim SG, Ugurbil K, et al. Magnetic field and tissue dependencies of human brain longitudinal 1H2O relaxation in vivo. Magn Reson Med. 2007;57(2):308–18.
13 Visser F, Zwanenburg JJ, Hoogduin JM, Luijten PR. High-resolution magnetization-prepared 3D-FLAIR imaging at 7.0 Tesla. Magn Reson Med. 2010;64(1):194–202.
14 Adriany G, Van de Moortele PF, Wiesinger F, Moeller S, Strupp JP, Andersen P, et al. Transmit and receive transmission line arrays for 7 Tesla parallel imaging. Magn Reson Med. 2005;53(2):434–45.
15 Gras V, Vignaud A, Amadon A, Le Bihan D, Boulant N. Universal pulses: A new concept for calibration-free parallel transmission. Magn Reson Med. 2017;77(2):635–643.
16 Faber J, Paech D, Pracht E, Stirnberg R, Ehses P, Völzke Y, et al. Ready for Routine: Homogeneous, High-Resolution, and Multicontrast Whole-Brain MRI at 7 Tesla in Short Scan Time With "plug-and-Play" pTx Sequences. Invest Radiol. 2025. doi: 10.1097/RLI.0000000000001252. Epub ahead of print.
17 Herrler J, Liebig P, Gumbrecht R, Ritter D, Schmitter S, Maier A, et al. Fast online-customized (FOCUS) parallel transmission pulses: A combination of universal pulses and individual optimization. Magn Reson Med. 2021;85(6):3140–3153.
18 Piredda GF, Sleight E, Yu T, Klauser A, Pato Montemayor N, Philippe J, et al. Individually optimized dynamic parallel transmit pulses for 3D high-resolution SPACE imaging at 7T. Magn Reson Med. 2025;94(4):1616–1625.

Contact

Emilie Sleight, Ph.D.
CIBM Center for Biomedical Imaging
EPFL Campus Biotech
Chemin des Mines 9
1202 Geneva
Switzerland
emilie.sleight@epfl.ch

Professor Frédéric Grouiller, Ph.D.
CIBM Center for Biomedical Imaging
Division of Radiology
Diagnostic Department
Geneva University Hospitals (HUG)
Boulevard de la Tour 8
1205 Geneva
Switzerland
frederic.grouiller@hug.ch

Professor Felix T. Kurz, M.D., Ph.D.
Division of Neuroradiology
Diagnostic Department
Geneva University Hospitals (HUG)
Rue Gabrielle-Perret-Gentil 4
1205 Geneva
Switzerland
FelixTobias.kurz@hug.ch